NUCL SCI TECH (2019) 30:92
https://doi.org/10.1007/s41365-019-0621-3

Calculation of dpa rate in graphite box of Tehran Research Reactor (TRR)

Mohamad Amin Amirkhani[1] · Mohsen Asadi Asadabad[1] · Mostafa Hassanzadeh[1] · Seyed Mohammad Mirvakili[1] · Ali Mohammadi[2]

Received: 16 October 2018 / Revised: 23 January 2019 / Accepted: 26 January 2019 / Published online: 15 May 2019

Abstract Radiation damage is an important factor that must be considered while designing nuclear facilities and nuclear materials. In this study, radiation damage is investigated in graphite, which is used as a neutron reflector in the Tehran Research Reactor (TRR) core. Radiation damage is shown by displacement per atom (dpa) unit. A cross section of the material was created by using the SPECOMP code. The concentration of impurities present in the non-irradiated graphite was measured by using the ICP-AES method. In the present study the MCNPX code had identified the most sensitive location for radiation damage inside the reactor core. Subsequently, the radiation damage (spectral-averaged dpa values) in the aforementioned location was calculated by using the SPECTER, SRIM Monte Carlo codes, and Norgett, Robinson and Torrens (NRT) model. The results of "Ion Distribution and Quick Calculation of Damage" (QD) method groups had a minor difference with the results of the SPECTER code and NRT model. The maximum radiation damage rate calculated for the graphite present in the TRR core was 1.567×10^{-8} dpa/s. Finally, hydrogen retention was calculated as a function of the irradiation time.

Keywords Radiation damage · Graphite · SPECTER · SRIM · MCNPX · Tehran Research Reactor

✉ Mohsen Asadi Asadabad
msasadi@aeoi.org.ir

[1] Reactor and Nuclear Safety Research School, Nuclear Science and Technology Research Institute, Tehran, Iran

[2] Department of Physics, Arak University, Arak, Iran

1 Introduction

Radiation (energetic gammas, neutrons, and other particles) is emitted during fission and fusion reactions which occur in nuclear reactors and throughout the process of radioactive decay. Primary Knock-on Atoms (PKAs) are created as a result of a collision between radiation atoms. Exposure to radiation can induce changes in material properties. The aforesaid changes are a function of the number of atoms that have been displaced from lattice equilibrium sites [1].

The main cause of damage in the environment of fission reactors is the displacement of atoms due to neutron collisions. Kinetic energy is transported to target atoms during neutron collision. As a result, pairs are created between the vacancy and interstitial atoms. They are called "Frenkel Pairs" (FPs). The FP formation time is about 10^{-11} s after the collision. Consequently, microstructure changes and defected clusters are created by the FPs. The formation of the defects stated above influences the chemical, mechanical, and other physical properties (growth, segregation, swelling, phase change, defect clustering, dissolution rate, and bubble formation) of irradiated materials [1–5].

Several methods are used to predict and compute the evolution, formation rate, and behavior of radiation damages, namely the binary collision approximation (BCA), the molecular dynamics (MD), and the kinetic Monte Carlo (KMC) methods [1]. Economical, safe, and reliable operation of nuclear power plants requires knowledge of the factors that may affect the material properties of the facility during its lifetime.

Graphite has been used in the nuclear industry from the time of establishment of the first critical reactors (Chicago pile-1) to fully commercialized reactors. It is used as a

reflector, moderator [6–8] in fission reactors, and divertor in plates [6, 9] of fusion reactors. Proper specification of graphite (high-temperature thermal properties, mechanical stability, superior moderation properties, easy machinability, cost-effectiveness, high scattering, and low neutron capture cross section) is identified as the reason behind its use as a structural material and moderator in nuclear reactors [10–13]. Large specification changes occur due to imposition of gross microstructure evolution under neutron irradiation [8, 14]. Although graphite has been used in the nuclear industry since the usage of the first graphite pile, there is a deficiency of holistic perception about its properties which is mainly due to the hardship associated with neutron irradiation experiments and its very complex microstructure [15].

The method for calculation of dpa in nuclear reactors is discussed in some papers [16, 17] where it is shown that atom displacement depends on the flux value and neutron spectrum [18, 19] of the materials, while other papers have shown the effects of neutron damage on graphite [20–25]. Wigner energy is created in graphite as a result of irradiation with neutrons in power and research reactors [26]. However, the aforementioned phenomenon is not the subject of this study. Graphite is used as a reflector to increase the neutron flux in TRR core [27]. These calculations are very important for the reactor safety, power plant management, and any experimental test.

The purpose of this paper is to estimate the radiation damage in dpa units, that is, the average number of times an atom is displaced from its lattice site during the period of irradiation [28]. Two codes were used for the aforesaid purpose, namely SRIM and SPECTER codes. In all techniques, MCNPX 2.6 code was used with ENDF/B-VI library to locate the region characterized by the maximum neutron flux in TRR core [29]. Following the calculation of neutron flux using the above-mentioned code, radiation damage in the graphite box (GR) was calculated by using the SRIM 2013 computer program which is developed by Biersack, Ziegler, and others. SRIM is a Monte Carlo software based on the BCA method. It can be used for simulating the ion and neutron irradiation experimentations. For simulating neutron irradiation, the SRIM code uses the file titled TRIM.DAT which contains the kinetic information (type, energy, collision position, and movement angle data) of PKAs. This file can be produced by the AMTRACK [30] code using the MCNPX code. A graphical user interface, a wide range of collision particles, and graphical output are the benefits of the SRIM code. The SRIM code can calculate the ion distribution, ionization, and energy lost by phonons at different depths of the target.

In the second method, an estimate of radiation damage was computed by using the SPECTER code and the result was compared with the previous method. This code was developed by Greenwood [31] to easily calculate the damage incurred by any specified neutron irradiation. Unlike the other code, which is used for computing dpa rate, this code uses the Monte Carlo method for computing the aforementioned parameter [32].

In the last method, NRT model was used to calculate the damage rate and the results were compared with those obtained through other methods. This model was developed by Norgett et al. [33] for calculating the damage rate of a PKA with a given energy. The international radiation effects community adopted the NRT model as a standard model for calculating damage rate [34].

In the final section of the article, hydrogen retention is obtained as a function of the irradiation time. The radiation damage rate in the Tehran reactor has been calculated for the first time. Due to the long life of the reactor, these calculations and establishment of a material specification database are essential for long-term management of the reactor.

2 Materials and methods

2.1 Dpa calculation

Tehran Research Reactor (TRR) is a 5-MW pool-type, light-water, moderated reactor. It is operated with U_3O_8 enrichment (20%) fuels chiefly for the purpose of research, training, irradiation experiments and production of radioisotopes. TRR core consists of two types of fuel assemblies, namely Standard Fuel Element (SFE) and Control Fuel Element (CFE). Nuclear-grade graphite which is protected by an external aluminum box (Gr) is used as a neutron reflector. Material irradiation is conducted in IR-Box positions [27]. Figure 1 shows a planar view of the TRR core configuration as simulated by the MCNPX code.

In the first method, SPECOMP 2002 code [35] was used to calculate the displacement cross section of graphite, while neutron flux was calculated by the MCNPX code. These results are used to evaluate the dpa by using the SPECTER code. In addition, material composition was also measured by using the inductively coupled plasma emission spectrometry (ICP-AES) method. The calculated composition was used as inputs for the MCNPX and SPECOMP codes. Figure 2 shows the flowchart of the radiation damage calculation process followed by the SPECTER code.

In the second method, neutron radiation damage on the graphite and rate of dpa are evaluated by using the SRIM/TRIM computer code. The SRIM code requires the kinetic information of the atoms for calculating neutron radiation damage. The latter is required to start the recoil cascades that should be extracted from the file titled TRIM.DAT.

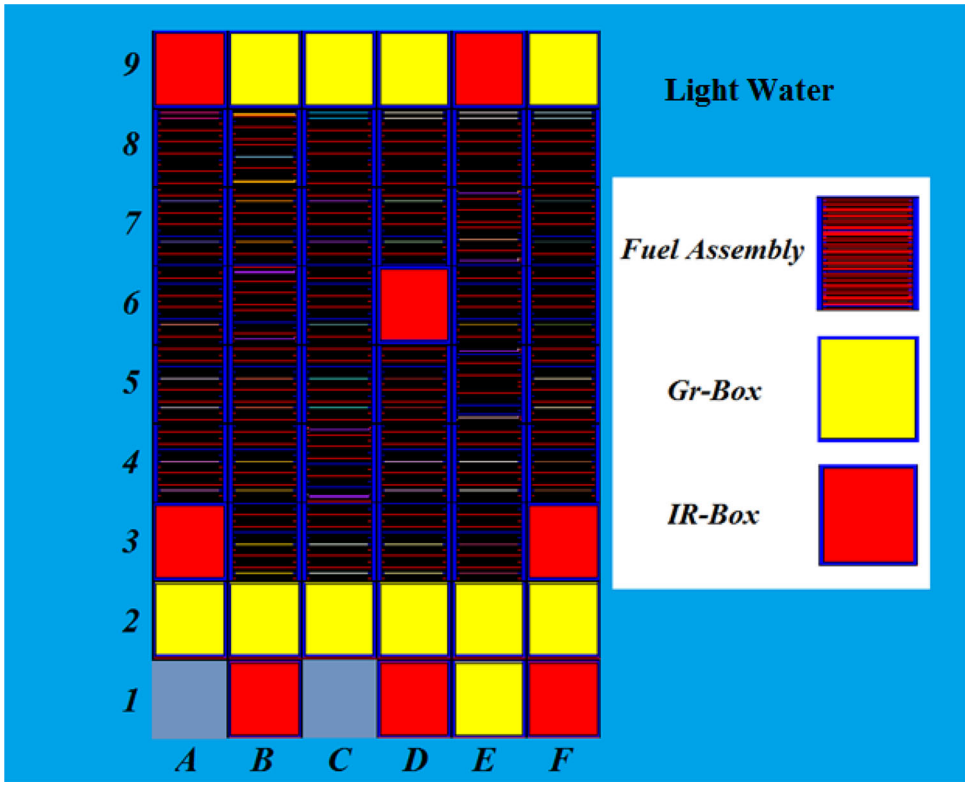

Fig. 1 (Color online) Planar view of the TRR core configuration in MCNPX code

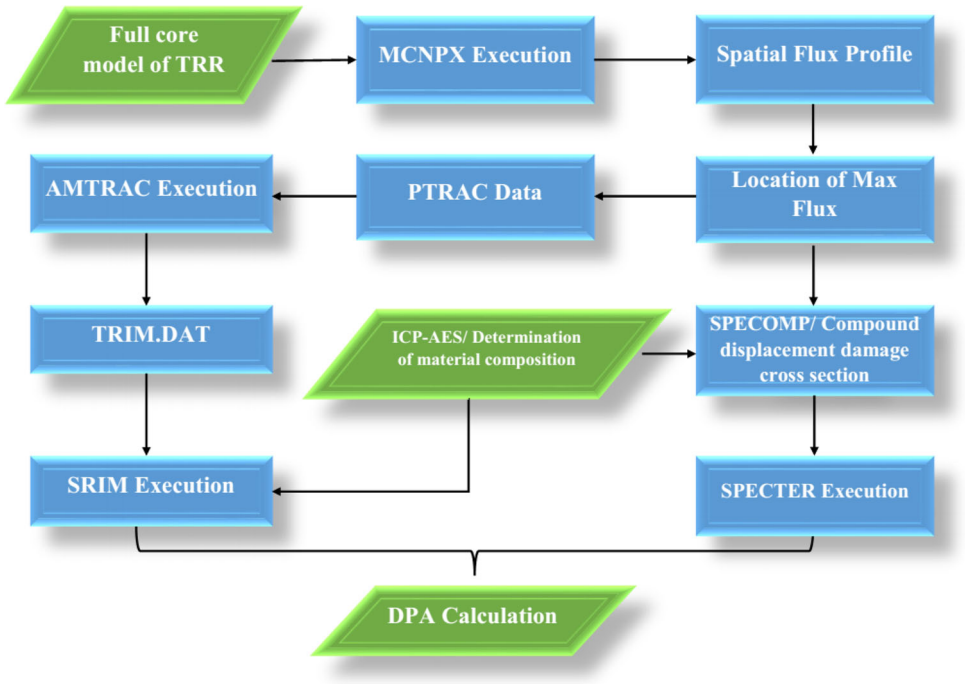

Fig. 2 Flowchart of radiation damage calculation process

AMTRACK is used to obtain the aforementioned file from the MCNPX-PTRAC (particle track) output file [30]. AMTRACK can reform the MCNPX-PTRAC output file whose code is written by using the MATLAB software [29]. PTRAC file has energy before and after collision, the particle type, position of reaction, reaction type, and movement angle data [29]. Flowchart of the radiation damage calculation process followed by the SRIM code is displayed in Fig. 2.

The concentration of impurities in the graphite before irradiation was measured through the ICP-AES (VARIAN, LIBERTY50AX TURBO, Australia) method. Type and amount of impurities were specified by using the X-ray fluorescence (XRF) method. For preparing the ICP-AES solution, 0.549 g of graphite powder was dissolved in 100 ml of p.a. grade 2% nitric acid (for 72 h). Nitric acid (2 vol%) was prepared by diluting 65% nitric acid manufactured by the Merck Company in distilled water. After dissolving the graphite powder sample in the acid, the solution was passed through a Whatman filter which was manufactured by the Sigma-Aldrich Company. The resulting solution was analyzed by using the ICP-AES [36]. The material composition of the sample is shown in Table 1.

After calculating the number of atom displacements from the SRIM code and the neutron flux from the MCNPX code, Eq. (1) can be used to calculate the damage rate in dpa/s unit:

$$R\left(\mathrm{dpa}/\mathrm{s}\right) = \frac{\varphi \times d}{A}, \tag{1}$$

where φ is the flux of neutron in n $(\mathrm{cm}^2\ \mathrm{s})^{-1}$ unit, d is the number of atom displacements in 1/(n cm) unit, and A is the atomic density expressed in at. cm^{-3} unit [37]. Atomic density for graphite is 1.122×10^{23} at. cm^{-3}. The total radiation damage can be calculated by using the following equation:

$$D(\mathrm{dpa}) = Rt, \tag{2}$$

where t(s) is the time of radiation.

2.2 Relationship between hydrogen retention and radiation

Hydrogen atoms may be trapped in two sites during the irradiation of graphite, namely interstitial cluster loop edge sites (trap 1) and carbon dangling bonds at edge surfaces of crystallites (trap 2). A study had shown that neutron irradiation creates 1 trap site at upper fluence with more than 0.017 dpa [25]. Hydrogen retention of neutron-irradiated graphite and the relationship between fluence (dpa) and hydrogen retention for the different kinds of trapping sites are shown for different neutron damages in Fig. 3. Using numerical interpolation, the relationship between fluence (dpa) and hydrogen retention (hydrogen retention per unit mass (H/C)) for different kinds of trapping sites can be obtained as follows:

$$H_{\mathrm{T}}\left(\frac{H}{C}\right) = 4 \times 10^{-4} \ln D + 3.1 \times 10^{-3}, \tag{3}$$

$$H_1\left(\frac{H}{C}\right) = 2 \times 10^{-4} \ln D + 1.3 \times 10^{-3}, \tag{4}$$

$$H_2\left(\frac{H}{C}\right) = 2 \times 10^{-4} \ln D + 1.8 \times 10^{-3}, \tag{5}$$

where D is radiation damage in dpa unit and H_{T}, H_1, H_2 are total hydrogen retention, hydrogen retention of trap 1 and trap 2, respectively.

3 Results and discussion

3.1 Calculation of neutron flux in GR-Box using MCNPX code

Like other transport codes, MCNPX uses the density of simulated objects to calculate the mean free path of the traced particles in the media and track them over a wide range of energies. The computational model was built as per the information available from the final safety analysis report (FSAR). The MCNPX code was used to simulate neutron transport in the core as well as to calculate neutron fluxes and neutron flux spectra [27, 29]. The reactor was critical, and control rods were 50% immersed into the core (core No. 83). The core contained 0.0435 ton of uranium. Considering the different burn-ups of each fuel assembly, different materials were recommended for each one of the assemblies used in the MCNPX simulation. Burn-up of each fuel assembly is shown in Fig. 4.

In addition, the flux of every graphite box was calculated by using F4 tally (track length estimate of cell flux) and it is shown in Fig. 4. In MCNPX code, F4 tally determines the flux in any given volume. This tally calculates the neutron flux through a certain area or the number of neutron in a particular energy interval. MCNPX tallies were normalized to per starting particle [29]. As seen in the figure, graphite box in C9 position has the maximum total flux which measures up to 6.46×10^{13} n/$(\mathrm{cm}^2\ \mathrm{s})$. Statistical uncertainties were less than 0.7% in the calculated fluxes.

Figure 5 shows the axial flux on C9 graphite box. It can be seen that higher neutron flux exists between a height of

Table 1 Material composition of graphite (amounts are in wt%, balance C*)

Element	Al*	Si*	Ca*	Na*	S	B	Fe
Graphite	0.311	0.306	0.331	0.084	0.026	4.86×10^{-3}	4.32×10^{-3}

*C, Al, Si Ca, and Na are used to model graphite with SPECOMP

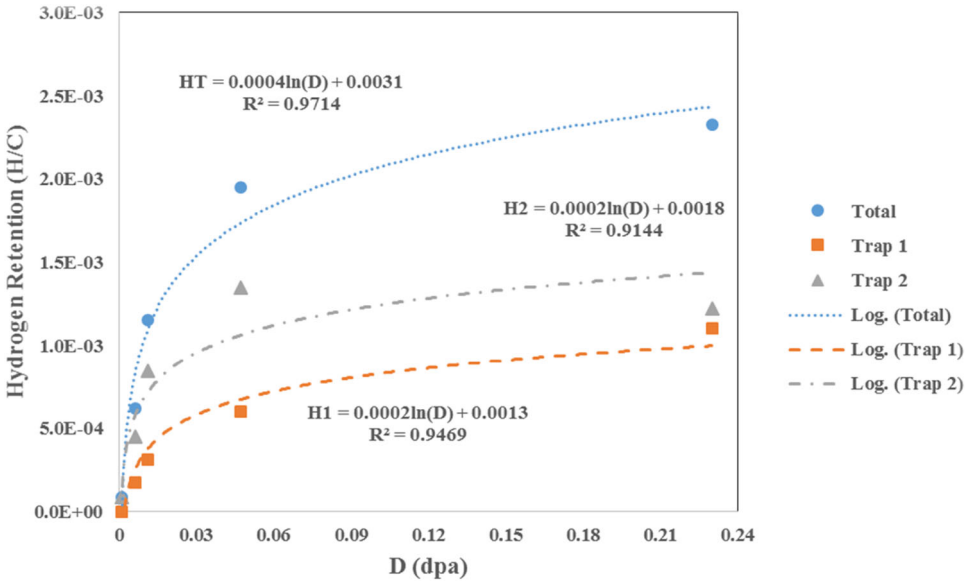

Fig. 3 (Color online) Hydrogen retention in neutron-irradiated graphite and the relationship between them shown for each trapping site

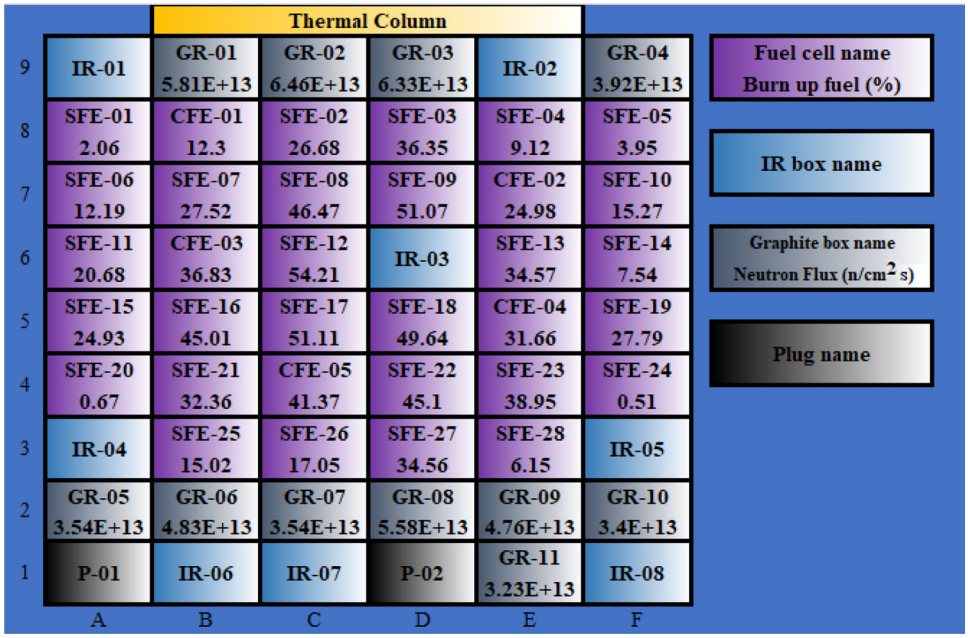

Fig. 4 (Color online) Flux on graphite boxes of TRR and burn-up of every fuel assembly for core No. 83

20 cm and 30 cm (about 8.5×10^{13} n/(cm^2 s)). Thus, this position was selected to calculate the radiation damage of GR-Box. Neutron spectrum (69 groups) was calculated by using F2 tally in MCNPX code, since this spectrum is suitable for simulation in TRR [27]. Spectrum was extracted from Ref. [38] to calculate dpa in graphite box. Additionally, peak flux was used on the graphite box surface to calculate the dpa caused by neutron encounter in the graphite box of TRR core. This computation was conducted by using Eq. 1.

3.2 Calculation of dpa rate using SPECOMP/SPECTER codes

Neutron radiation damage can simply be calculated by using the SPECTER computer code for any specified neutron irradiation. In the aforementioned code, recoil spectra, total damage energy (kerma), and gas production are computed, too. The library files of the SPECTER code are very extensive. The dpa cross section for new material can be calculated by using SPECOMP code. It is appended to COMPOUND.DAT file. SPECOMP can be utilized for the materials which have five of the 38 elements contained in the SPECTER code [35]. The material composition of

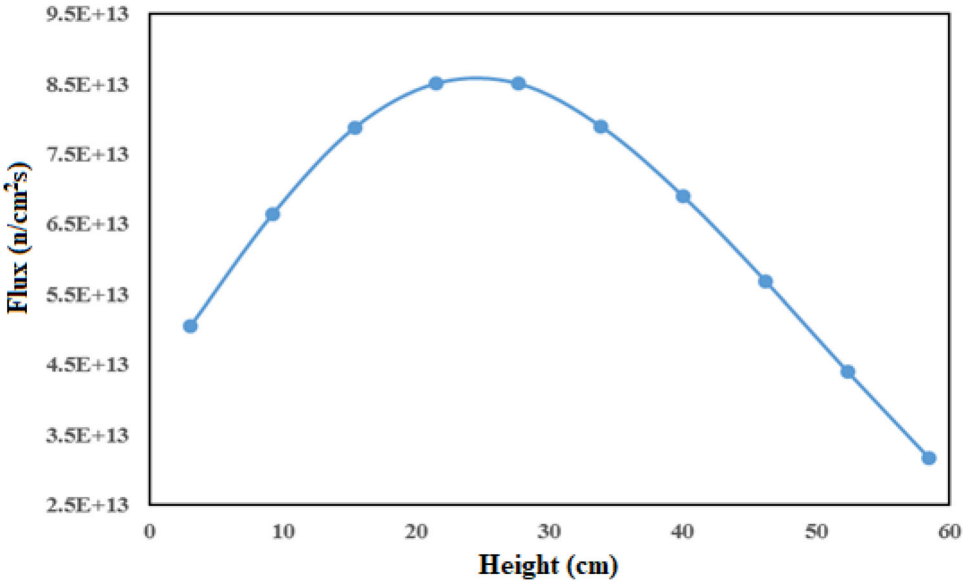

Fig. 5 Axial flux on C9 graphite box

graphite is presented in Table 1. It should be noted that only C, Al, Si, Ca, and Na elements are chosen to model graphite in the SPECOMP code. Figure 6 shows the displacement cross section for graphite that has been calculated by using the SPECOMP code. The physical parameters which were used in the SPECOMP code are shown in Table 2. MCNPX code was used to evaluate the neutron flux on the graphite box surface. Consequently, the peak flux area was specified. Finally, the SPECTER code was used to calculate the dpa rate.

3.3 Calculation of dpa rate using SRIM/TRIM code

Ion distribution profiles of material irradiation can be calculated by using the SRIM (also known as TRIM) which is a Monte Carlo simulation code. Degree of ion penetration in a material is calculated through the binary collision approximation (BCA) method in the SRIM. SRIM code uses material composition and density for describing a material. The TRIM.DAT file contains the kinetic information of atoms, and it starts recoil cascades in neutron damage simulation [32].

An element with $1 \times 1 \times 1$ cm^3 dimensions (target) was utilized to extract PTRAC file from the MCNPX code. The file contains data about energies before and after the collision, the particle type, position, and type of reaction as well as movement angle. The aforesaid information was utilized for calculating the dpa using the SRIM code. Figure 7 shows the neutron spectrum output of the target.

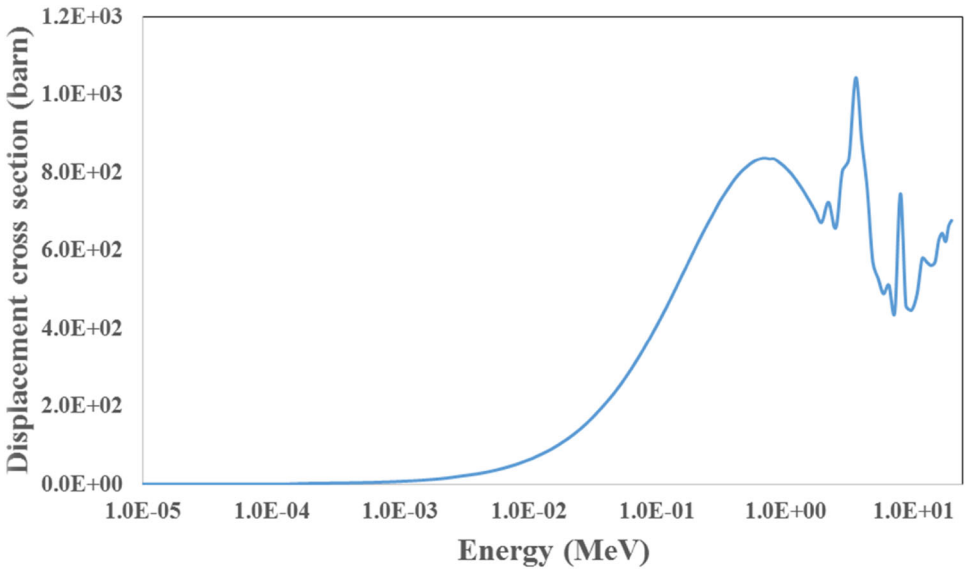

Fig. 6 Displacement cross section of graphite as calculated by the SPECOMP code

Table 2 Physical parameters used for performing SPECOMP calculation on recoils of neutrons in graphite

Parameter	C [32]	Al [39]	Si [40]	Ca [41]	Na [41]
Displacement energy (eV)	28	25	15	40	25
Effective gamma damage energy (eV)	671	674	596	388	618

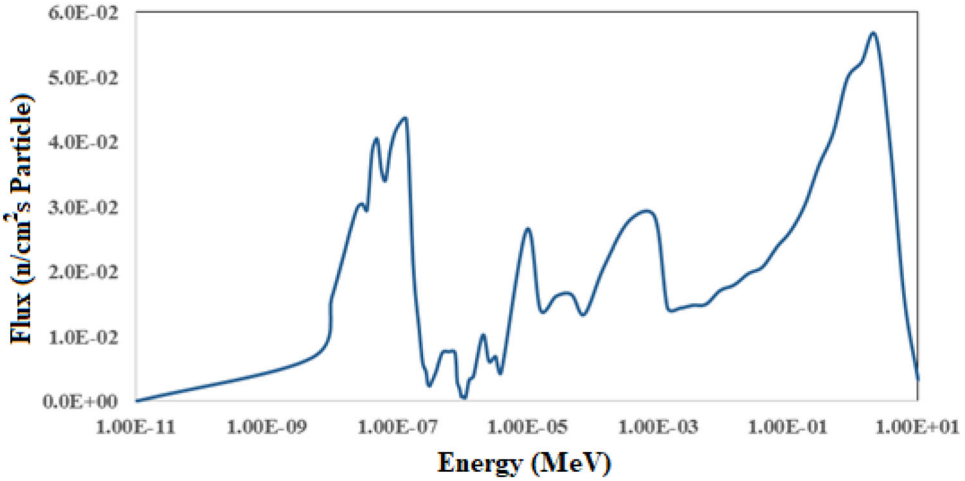

Fig. 7 Neutron spectrum output of the target

Table 3 Nuclear reaction in the material

Target atom	Reaction and production	Un-normalized production (at. $cm^{-3}s$)
C	^{12}C (n, γ)^{13}C	8.39×10^{-5}
	^{12}C (n, α)^{9}Be	4.93×10^{-5}
	^{13}C (n, γ)^{14}N	3.66×10^{-7}

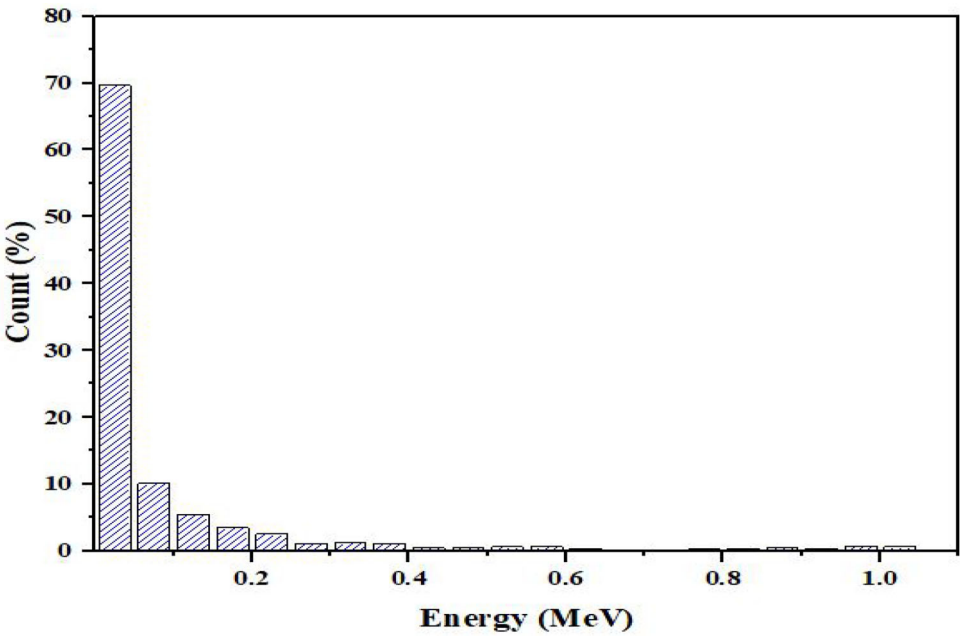

Fig. 8 PKA spectrum used in SRIM calculation

Table 3 demonstrates the nuclear reaction occurring in the specimen. Transmutation reactions, ^{12}C (n, γ) ^{13}C and ^{13}C (n, γ) ^{14}N, occur due to thermal neutron capture, while ^{12}C (n, α) ^{9}Be reaction is performed for releasing high-energy neutron ($E > 7$ MeV) [42].

Table 4 Physical parameters used for SRIM simulation of recoils from neutrons in graphite

Parameter	Fe [39]	Al [39]	Ca [41]	Si [40]	S [41]	Na [41]	B [41]	C [32]
Lattice binding energy (eV)	3	3	3	2	3	3	3	3
Surface binding energy (eV)	4.34	3.36	1.83	4.7	2.88	1.12	5.73	7.41
Displacement energy (eV)	40	25	40	15	25	25	25	28

Table 5 Comparison of the rates of dpa calculated by SPECTER, TRIM codes and NRT model

Code/model		Damage level (vacancies/ion)	Damage rate (dpa/s)	dpa/EFPD*
SRIM 2013	QD	171	1.567×10^{-8}	1.3538×10^{-3}
SPECTER		–	1.507×10^{-8}	1.3020×10^{-3}
NRT		175	1.603×10^{-8}	1.3849×10^{-3}

*Effective full-power day

Table 6 Output parameters of SRIM

Parameter	QD
Total displacements (dpa/s)	1.567×10^{-8}
Total vacancies (dpa/s)	1.567×10^{-8}
Replacement collisions (dpa/s)	0
Total ionization (keV/PKA)	17,244.4
Total phonons (keV/PKA)	2642.1

PTRAC file was used to create TRIM.DAT file using AMTRACK (intermediate computer program). The latter is needed to simulate neutron radiation damage while using the SRIM code. Finally, SRIM uses the above-mentioned file along with the material composition (Table 1) information to calculate the dpa. Figure 8 shows the PKA spectrum which is calculated by AMTRACK. Simulation is performed by approximately 100,000 ions.

SRIM has two methods for simulating the radiation damage evolution, namely "Ion Distribution and Quick Calculation of Damage" (QD) and "Detailed Calculation with Full Damage Cascades" (FC). In the QD method, the code uses the Kinchin–Pease equation for estimating the number of defects on each Primary Knock-on Atom based on its recoil energy and the trajectories of primary ions only. Subsequently, Primary Knock-on Atoms (PKAs) are produced. In the FC method, the total collision cascade is calculated for less than 1 eV energy by applying the BCA. In addition, track of all displaced atoms and their count are also evaluated. In this method, "replacement collisions" reduce the vacancy number [43, 44]. Studies have shown that the QD method has more reliable results [45].

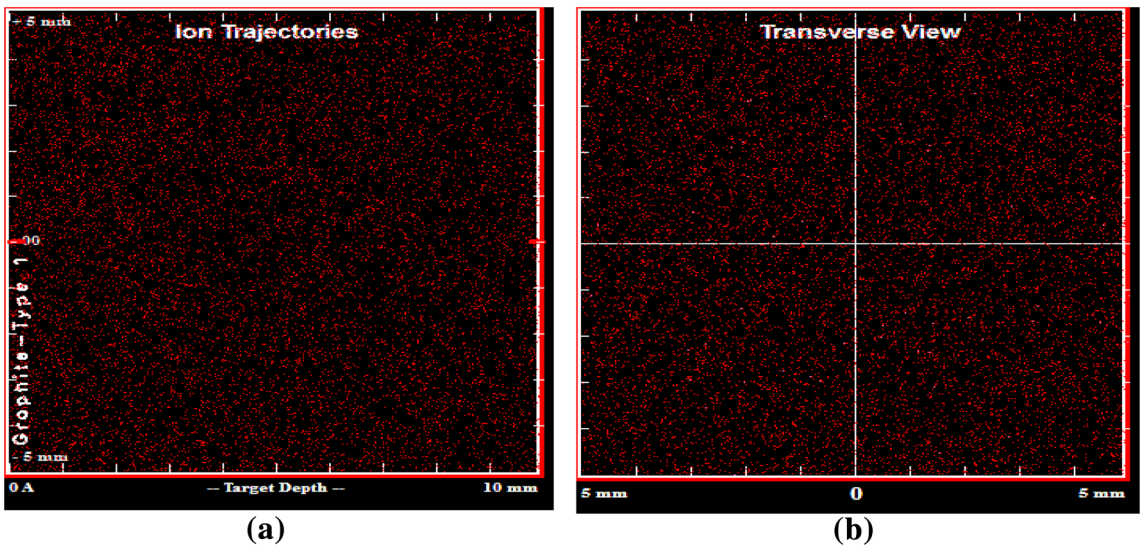

Fig. 9 (Color online) **a** PKAs trajectory and **b** transverse view of the neutron spectrum of 69 groups which was considered during the QD method

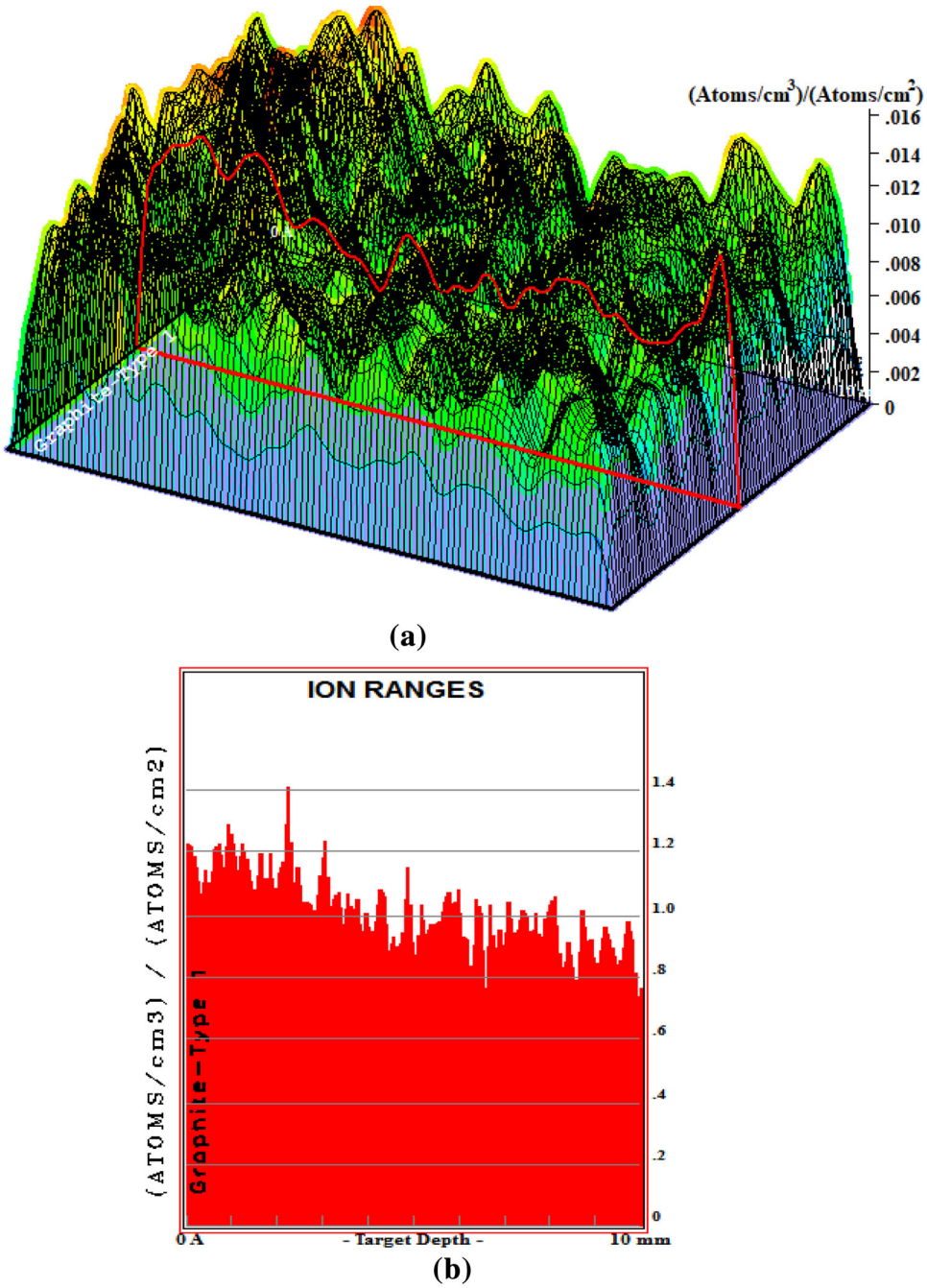

Fig. 10 (Color online) **a** PKAs distribution (3D) and **b** PKAs ranges for all neutrons that had stopped within the graphite during the QD method

The physical parameters which were used for SRIM simulation are shown in Table 4. Lattice binding energy is the energy that every recoiling target atom loses when it leaves its lattice site and recoils in the target. Surface binding energy is the energy that target atoms must absorb to leave the surface of the target, and displacement energy (E_d) is the minimum energy that an atom needs to be displaced from its lattice site [32]. If the lattice atom receives less than E_d energy, the struck atom undergoes large amplitude vibrations within its site but remains in its location and vacancy is not created [17].

Table 5 shows the comparison of the rate of dpa in the SPECTER and SRIM codes. The obtained results are also compared with the ones derived from the NRT method. The calculation procedure used in the NRT method had been discussed by Stoller et al. [45] and Saha et al. [28]. The rate of damage incurred while conducting the reactor function on full power for 1 day had been obtained. The

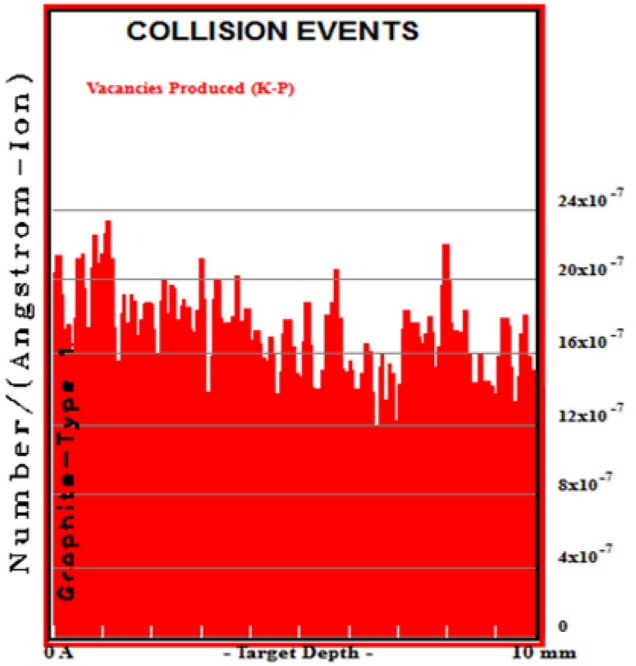

Fig. 11 Production of vacancies as calculated by applying the QD method on the graphite

results obtained from the two codes and the NRT method were consistent with each other. Similar results had been obtained in the previous researches [44]. The results obtained through the QD method had a lower difference with the results derived from the SPECTER code and the NRT method. The QD and NRT methods for graphite calculated a damage level of about 171 vacancies/ion and 175 vacancies/ion, respectively.

The QD mode calculated a damage rate of 1.567×10^{-8} dpa/s, while the dpa calculated by the QD mode for one effective full-power day (EFPD) was 1.3538×10^{-3} displacements. The SPECTER code calculated 1.507×10^{-8} dpa/s as the rate of damage, and the dpa/EFPD equaled 1.302×10^{-3} displacements. Through the NRT method, the values of 1.603×10^{-8} dpa/s and 1.3849×10^{-3} were obtained for the damage rate and dpa/EFPD, respectively.

Table 6 presents the output parameters of the SRIM code. Displacement occurs when the energy of struck atom (E_2) is greater than the displacement energy (E_d). "Total displacements" is equal to the total rate of these displacements. If both atoms (incident and struck atoms) have enough energy ($E_1 > E_d$ & $E_2 > E_d$) to leave the lattice site, a vacancy is created. The "total vacancies" parameter shows the total number of the vacancies mentioned earlier. "Replacement collisions" is the rate with which incident atom ejects struck atom from the original lattice site and stays in its location. "Total ionization" is the energy lost by electrons. In addition, "total phonons" expresses the energy lost by the target phonons [32].

Figure 9 presents the "PKAs trajectory" and "transverse view" of neutron spectrum of 69 groups which was considered for QD method. Figure 10 shows the "PKAs distribution" and "PKAs ranges" for all PKAs in the neutron spectrum of 69 groups, that had stopped within the graphite during the QD method. Figures 9 and 10 illustrate a nearly uniform PKAs distribution. The lack of peak in the distribution of PKAs in material causes a uniform change in the material specification. The uniform distribution was consistent with the results stated in reference [1].

Figure 11 shows the vacancy distributions calculated by using the SRIM code. Figure 12 shows the total displacements and vacancy distributions per ion collision in 3D which were derived from neutron spectrum of 69 groups. A nearly uniform area was obtained for vacancy and atom distributions. The aforesaid observation is consistent with previous researches. Uniform distribution is created by collisions of neutron with atoms [1]. The QD method for graphite had obtained a damage rate of 1.567×10^{-8} dpa/s, and the dpa calculated through the QD method for one effective full-power day (EFPD) was 1.3538×10^{-3} displacements.

3.4 Hydrogen retention calculation

Figure 13 illustrates the dependency of hydrogen retention on the irradiation time for the different types of trapping sites. The starting point for the trapping of hydrogen in interstitial cluster loop edge sites is after about one day of irradiation. As visible in the figure, the hydrogen trapping begins to saturate after a time. These results are similar to the ones obtained by other researches [9, 25].

4 Conclusion

In this study, the core of TRR was simulated by using MCNPX code and the location with the highest neutron flux was identified. The radiation damage rate in the Tehran reactor was calculated for the first time. The calculation of the radiation damage rate is essential for any empirical assay in this field. In the case of the aforementioned location, the dpa value was estimated for the graphite box using SPECTER and SRIM codes as well as the NRT method for neutron spectrum of 69 groups. The material composition of graphite was measured using the ICP-AES

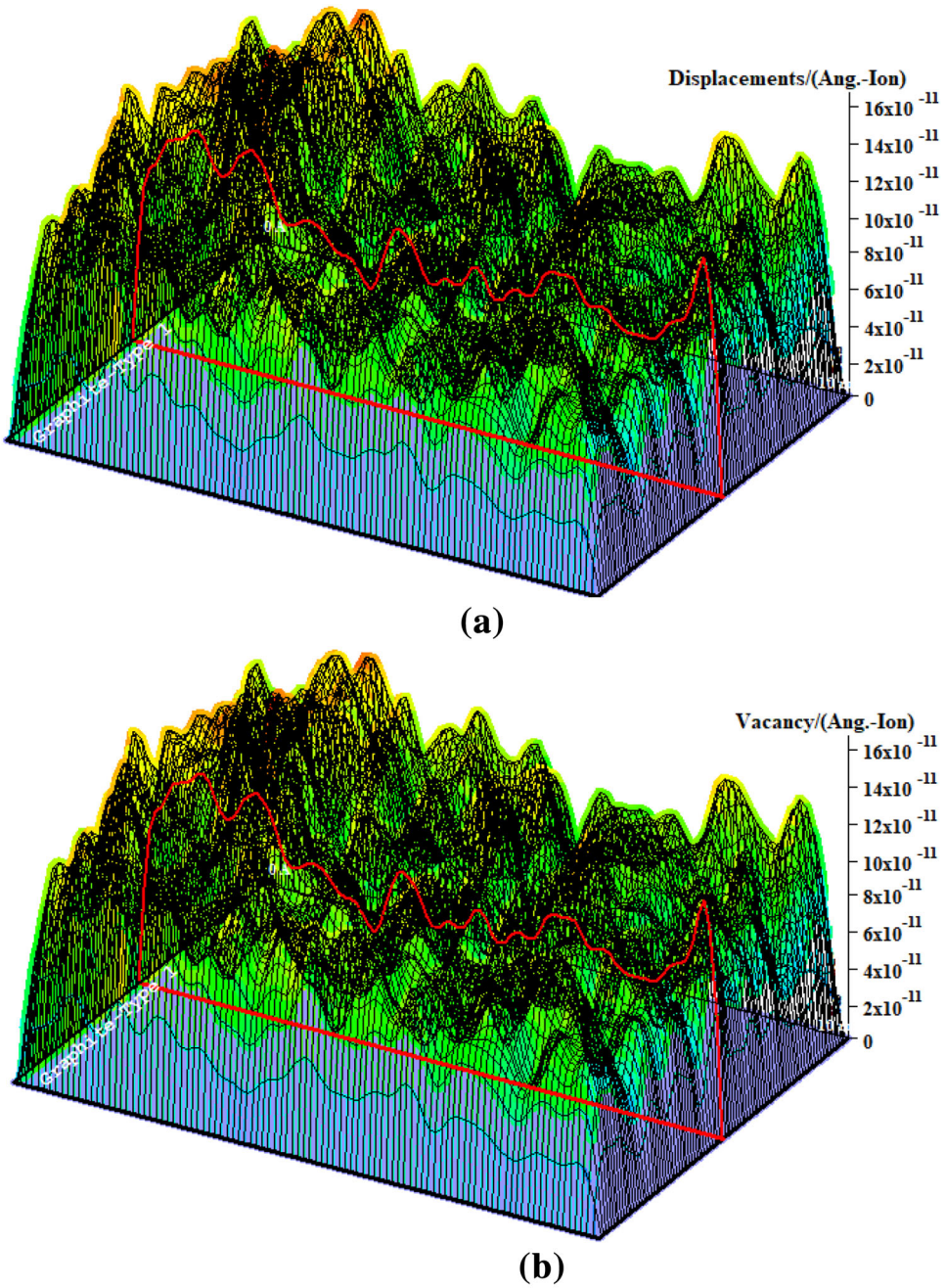

Fig. 12 (Color online) **a** Total displacements and **b** total vacancy distributions within the graphite obtained from the QD method

method, and it was used in the above-listed codes. The results obtained through the "Quick Calculation of Damage" method by using SRIM code were in agreement with the SPECTER and NRT model results. The maximum radiation damage rate of 1.567×10^{-8} dpa/s was obtained for graphite in TRR core. These results serve as evidence to the almost uniform distribution of PKAs in the material, which causes a uniform change in the material specification in neutron radiation. Using the experimental data, the equation for hydrogen retention changes was also obtained. Dependency of hydrogen retention on the irradiation time was calculated for the different types of trapping sites present in the environmental conditions of the Tehran reactor. It was observed that hydrogen retention begins to saturate after a certain period of time. This observation is similar to the results of other studies.

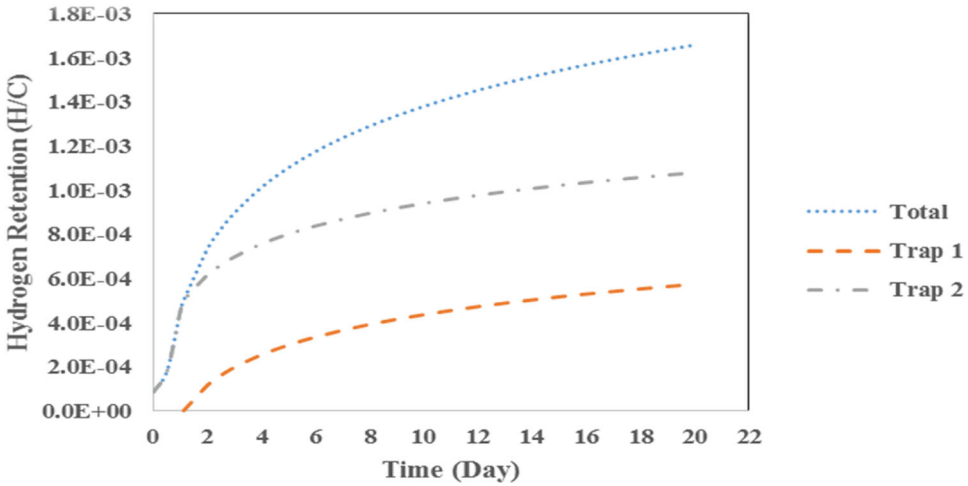

Fig. 13 Dependency of hydrogen retention on the time of irradiation

References

1. G.S. Was, *Fundamentals of Radiation Materials Science: Metals and Alloys* (Springer, Berlin, 2007)
2. D.G. Cacuci, *Handbook of Nuclear Engineering: Vol. 1: Nuclear Engineering Fundamentals; Vol. 2: Reactor Design; Vol. 3: Reactor Analysis; Vol. 4: Reactors of Generations III and IV; Vol. 5: Fuel Cycles, Decommissioning, Waste Disposal and Safeguards. Vol. 2* (Springer, Berlin, 2010)
3. G.Y. Wu, N.W. Hu, H.Q. Deng et al., Simulation of radiation damages in molybdenum by combining molecular dynamics and OKMC. Nucl. Sci. Tech. **28**, 3 (2017). https://doi.org/10.1007/s41365-016-0164-9
4. Y. Yang, Y.W. Su, W.Y. Li et al., Evaluation of radiation environment in the target area of fragment separator HFRS at HIAF. Nucl. Sci. Tech. **29**, 147 (2018). https://doi.org/10.1007/s41365-018-0479-9
5. S.A. Fabritsiev, A.S. Pokrovsky, S.J. Zinkle et al., The effect of neutron spectrum on the mechanical and physical properties of pure copper and copper alloys. J. Nucl. Mater. **233**, 526–533 (1996). https://doi.org/10.1016/S0022-3115(96)00260-7
6. C. Hubert, K.O. Voss, M. Bender et al., Swift heavy ion-induced radiation damage in isotropic graphite studied by micro-indentation and in situ electrical resistivity. Nucl. Instrum. Methods B **365**, 509–514 (2015). https://doi.org/10.1016/j.nimb.2015.08.056
7. B.T. Kelly, Graphite—the most fascinating nuclear material. Carbon **20**, 3–11 (1982). https://doi.org/10.1016/0008-6223(82)90066-5
8. B.T. Kelly, *Physics of Graphite* (Applied Science, London, 1981), p. 267
9. H. Atsumi, T. Tanabe, T. Shikama, Bulk hydrogen retention in neutron-irradiated graphite at elevated temperatures. J. Nucl. Mater. **390**, 581–584 (2009). https://doi.org/10.1016/j.jnucmat.2009.01.112
10. T.R. Allen, K. Sridharan, L. Tan et al., Materials challenges for generation IV nuclear energy systems. Nucl. Technol. **162**, 342–357 (2008). https://doi.org/10.13182/NT08-A3961
11. R. Nightingale, *Graphite in Nuclear Industry* (Academic Press, New York, 1962)
12. P.A. Thrower, W.N. Reynolds, Microstructural changes in neutron-irradiated graphite. J. Nucl. Mater. **8**, 221–226 (1963). https://doi.org/10.1016/0022-3115(63)90037-0
13. G. Ramos, B.M.U. Scherzer, Radiation damage, trapping and release of deuterium in diamond and HOPG-graphite. Nucl. Instrum. Methods B **174**, 329–336 (2001). https://doi.org/10.1016/S0168-583X(00)00590-5
14. S.P. Jing, C. Zhang, J. Pu et al., 3D microstructures of nuclear graphite: IG-110, NBG-18 and NG-CT-10. Nucl. Sci. Tech. **27**, 66 (2016). https://doi.org/10.1007/s41365-016-0071-0
15. C. Karthik, J. Kane, D.P. Butt et al., Neutron irradiation induced microstructural changes in NBG-18 and IG-110 nuclear graphites. Carbon **86**, 124–131 (2015). https://doi.org/10.1016/j.carbon.2015.01.036
16. O. Noorikalkhoran, I. Sevostianov, Micromechanical modeling of neutron irradiation induced changes in yield stress and electrical conductivity of zircaloy. Int. J. Eng. Sci. **120**, 119–128 (2017). https://doi.org/10.1016/j.ijengsci.2017.07.002
17. D. Saad, H. Nenkharfia, M. Izerrouken et al., Displacement damage cross section and mechanical properties calculation of an Es-Salam research reactor aluminum vessel. Nucl. Sci. Technol. **28**, 162 (2017). https://doi.org/10.1007/s41365-017-0319-3
18. U. Saha, K. Devan, A. Bachchan et al., Neutron radiation damage studies in the structural materials of a 500 MWe fast breeder reactor using DPA cross-sections from ENDF/B-VII. 1. Pramana **90**, 46 (2018). https://doi.org/10.1007/s12043-018-1536-y
19. D. Guo, C. He, H. Zang et al., Re-evaluation of neutron displacement cross sections for silicon carbide by a Monte Carlo approach. J. Nucl. Sci. Technol. **53**, 161–172 (2016). https://doi.org/10.1080/00223131.2015.1028502
20. H. Atsumi, M. Iseki, T. Shikama, Hydrogen behavior in carbon-based materials and its neutron irradiation effect. J. Nucl. Mater. **233**, 1128–1132 (1996). https://doi.org/10.1016/0022-3115(95)00180-8
21. H.M. Freeman, A.N. Jones, M.B. Ward et al., On the nature of cracks and voids in nuclear graphite. Carbon **103**, 45–55 (2016). https://doi.org/10.1016/j.carbon.2016.03.011
22. T. Burchell, Neutron irradiation damage in graphite and its effects on properties, in *Proceedings Carbon'02* (2002), pp. 15–19
23. C. Goodwin, A. Barkatt, M. Al-Sheikhly, On the mechanism of the interactions of neutrons and gamma radiation with nuclear graphite—implications to HTGRs. Radiat. Phys. Chem. **97**, 38–47 (2014). https://doi.org/10.1016/j.radphyschem.2013.10.021
24. R. Takahashi, M. Toyahara, S. Maruki, et al., Investigation of morphology and impurity of nuclear grade graphite, and leaching

mechanism of carbon-14, in *Proceedings of the Nuclear Graphite Waste Management* (1999), pp. 18–20
25. H. Atsumi, A. Muhaimin, T. Tanabe et al., Hydrogen trapping in neutron-irradiated graphite. J. Nucl. Mater. **386**, 379–382 (2009). https://doi.org/10.1016/j.jnucmat.2008.12.135
26. J. Rees, S. Assurance, *Wigner Energy in Irradiated Graphite and Post-Closure Safety: R&D Technical Report P3-80/TR* (Environment Agency, Bristol, 2002)
27. N.S.T.R. Institute, *Final Safety Analyses Report for Tehran Research Reactor* (Atomic Energy Organization of Iran, Tehran, 2009)
28. U. Saha, K. Devan, S. Ganesan, A study to compute integrated dpa for neutron and ion irradiation environments using SRIM-2013. J. Nucl. Mater. **503**, 30–41 (2018). https://doi.org/10.1016/j.jnucmat.2018.02.039
29. D.B. Pelowitz, *MCNPX 2.6.0 Manual, LANL, LA-CP-07-1473* (Los Alamos National Laboratory, Santa Fe, 2008)
30. A. Mohammadi, S. Hamidi, M.A. Asadabad, The use of the SRIM code for calculation of radiation damage induced by neutrons. Nucl. Instrum. Methods B **412**, 19–27 (2017). https://doi.org/10.1016/j.nimb.2017.08.036
31. L.R. Greenwood, R.K. Smither, *SPECTER: Neutron Damage Calculations for Materials Irradiations* (Argonne National Lab, Lemont, 1985)
32. J.F. Ziegler, J.P. Biersack, *SRIM-2008: Stopping power and range of ions in matter* (2008)
33. M.J. Norgett, M.T. Robinson, I.M. Torrens, A proposed method of calculating displacement dose rates. Nucl. Eng. Des. **33**, 50–54 (1975). https://doi.org/10.1016/0029-5493(75)90035-7
34. R. Stoller, G. Odette, Recommendations on damage exposure units for ferritic steel embrittlement correlations. J. Nucl. Mater. **186**, 203–205 (1992). https://doi.org/10.1016/0022-3115(92)90335-I
35. L.R. Greenwood, SPECOMP calculations of radiation damage in compounds. In *Reactor Dosimetry: Methods, Applications, and Standardization* (ASTM International, 1989)
36. R. Plukienė, A. Plukis, A. Plzas et al., Modelling of impurity activation in the RBMK reactor graphite using MCNPX. Prog. Nucl. Sci. Technol. **2**, 421–426 (2011). https://doi.org/10.15669/pnst.2.421
37. S.F.G. Ardekani, K. Hadad, Evaluation of radiation damage in belt-line region of VVER-1000 nuclear reactor pressure vessel. Prog. Nucl. Energy **99**, 96–102 (2017). https://doi.org/10.1016/j.pnucene.2017.05.00
38. W. Dorchester, RSICC COMPUTER CODE COLLECTION WIMS-D4, in *Atomic Energy Establishment* (1990)
39. ORNL, WIMS, *D4: Winfrith Improved Multigroup Scheme Code System* (Code CCC-575 Oak Ridge National Laboratory, Oak Ridge, TN, 1991)
40. I. Santos, L.A. Marqués, L. Pelaz, Modeling of damage generation mechanisms in silicon at energies below the displacement threshold. Phys. Rev. B **74**, 174115 (2006). https://doi.org/10.1103/PhysRevB.74.174115
41. Y. Iwamoto, H. Iwamoto, M. Harada et al., Calculation of displacement cross-sections for structural materials in accelerators using PHITS event generator and its applications to radiation damage. J. Nucl. Sci. Technol. **51**, 98–107 (2014). https://doi.org/10.1080/00223131.2013.851042
42. D.W. Muir, R.M. Boicourt, A.C. Kahler, *The NJOY Nuclear Data Processing System, Version 2012* (Los Alamos National Laboratory, Santa Fe, 2012)
43. G. Kinchin, R. Pease, The displacement of atoms in solids by radiation. Rep. Prog. Phys. **18**, 1 (1955). https://doi.org/10.1088/0034-4885/18/1/301
44. S.F.G. Ardekani, K. Hadad, Monte Carlo evaluation of neutron irradiation damage to the VVER-1000 RPV. Nucl. Energy Technol. **3**, 73–80 (2017). https://doi.org/10.1016/j.nucet.2017.04.001
45. R.E. Stoller, M.B. Toloczko, G.S. Was et al., On the use of SRIM for computing radiation damage exposure. Nucl. Instrum. Methods Phys. Res. Sect. B **310**, 75–80 (2013). https://doi.org/10.1016/j.nimb.2013.05.008